ESC HEART FAILURE
ESC Heart Failure 2020; **7**: 2113–2122
Published online 8 July 2020 in Wiley Online Library (wileyonlinelibrary.com) **DOI:** 10.1002/ehf2.12794

ORIGINAL RESEARCH ARTICLE

Tenascin-C aggravates ventricular dilatation and angiotensin-converting enzyme activity after myocardial infarction in mice

David Santer[1,2,3], Felix Nagel[1,2,4], Inês Fonseca Gonçalves[1,2], Christoph Kaun[5], Johann Wojta[1,5], Miklós Fagyas[6], Martin Kršśák[7], Ágnes Balogh[6], Zoltán Papp[6], Attila Tóth[6], Viktor Bánhegyi[6], Karola Trescher[1,2,4], Attila Kiss[1,2] and Bruno K. Podesser[1,2,4]*

[1]*Ludwig Boltzmann Institute for Cardiovascular Research, Medical University of Vienna, Waehringer Guertel 18-20, 1Q, Vienna, 1090, Austria;* [2]*Center for Biomedical Research, Medical University of Vienna, Vienna, Austria;* [3]*Department of Cardiac Surgery, University Hospital of Basel, Basel, Switzerland;* [4]*Department of Cardiac Surgery, Karl Landsteiner Private University for Health Sciences, St. Pölten, Austria;* [5]*Department of Internal Medicine II, Division of Cardiology, Medical University of Vienna, Vienna, Austria;* [6]*Division of Clinical Physiology, Department of Cardiology, Research Centre for Molecular Medicine, Faculty of Medicine, University of Debrecen, Debrecen, Hungary;* [7]*Department of Internal Medicine III, Division of Endocrinology and Metabolism, Medical University of Vienna, Vienna, Austria*

Abstract

Aims Tenascin-C (TN-C) is suggested to be detrimental in cardiac remodelling after myocardial infarction (MI). The aim of this study is to reveal the effects of TN-C on extracellular matrix organization and its haemodynamic influence in an experimental mouse model of MI and in myocardial cell culture during hypoxic conditions.

Methods and results Myocardial infarction was induced in TN-C knockout (TN-C KO) and wild-type mice. Six weeks later, cardiac function was studied by magnetic resonance imaging and under isolated working heart conditions. Myocardial mRNA levels and immunoreactivity of TN-C, TIMP-1, TIMP-3, and matrix metalloproteinase (MMP)-9, as well as serum and tissue activities of angiotensin-converting enzyme (ACE), were determined at 1 and 6 weeks after infarction. Cardiac output and external heart work were higher, while left ventricular wall stress and collagen expression were decreased ($P < 0.05$) in TN-C KO mice as compared with age-matched controls at 6 weeks after infarction. TIMP-1 expression was down-regulated at 1 and 6 weeks, and TIMP-3 expression was up-regulated at 1 week ($P < 0.01$) after infarction in knockout mice. MMP-9 level was lower in TN-C KO at 6 weeks after infarction ($P < 0.05$). TIMP-3/MMP-9 ratio was higher in knockout mice at 1 and 6 weeks after infarction ($P < 0.01$). ACE activity in the myocardial border zone (i.e. between scar and free wall) was significantly lower in knockout than in wild-type mice 1 week after MI ($P < 0.05$).

Conclusions Tenascin-C expression is induced by hypoxia in association with ACE activity and MMP-2 and MMP-9 elevations, thereby promoting left ventricular dilatation after MI.

Keywords Tenascin-C; Heart failure; Myocardial infarction; Isolated working heart; Mouse model; Extracellular matrix

Received: 21 February 2020; Revised: 8 May 2020; Accepted: 13 May 2020
**Correspondence to: Bruno K. Podesser, Ludwig Boltzmann Institute for Cardiovascular Research, Medical University of Vienna, Waehringer Guertel 18-20, 1Q, 1090 Vienna, Austria. Tel: +43 1 40400 52230; Fax: +43 1 40400 52290. Email: bruno.podesser@meduniwien.ac.at*

Introduction

Coronary artery disease is a major burden in the Western world. Myocardial infarction (MI) and subsequent left ventricular (LV) remodelling of the damaged myocardium deteriorate progressively because of the expanding scar. It can be described as a combination of volume and pressure overload, as the non-infarcted myocardium undergoes significant changes to maintain cardiac function.[1]

The extracellular matrix (ECM) protein tenascin-C (TN-C) is not expressed in the adult heart under physiological conditions (except in the chordae tendineae) but re-appears under pathological conditions such as dilated cardiomyopathy, myocarditis, or MI.[2,3] In line with that, the rapid accumulation of

TN-C, within 48 h, during acute inflammation at the edge of the necrotic tissue was observed.[4] Notably, in transmural MI, TN-C is up-regulated in the border zone, while it is expressed throughout the tissue in non-transmural MIs. Four weeks after MI, TN-C disappears from the scar, while TN-C expression sustains hibernating myocardium,[3,5] which underlines its role in cardiac remodelling. Conversely, TN-C knockout (KO) mice subjected to transverse aortic constriction showed a significant reduction in LV remodelling when compared with wild-type (WT) mice. This was accompanied by reduced LV and myocyte hypertrophy, less interstitial fibrosis, and reduced expression of matrix metalloproteinase (MMP)-2 and MMP-9 expression.[6] More recently, our group demonstrated that TN-C mRNA is up-regulated after MI in the border and infarcted zones, accompanied with a significant increase of plasma TN-C in a rat model of MI.[7] In line with that, Imanaka-Yoshida *et al.*[8] described that ischaemia induced mRNA expression of TN-C within 24 h, which peaks on Day 5 and ultimately diminishes around Day 14. Patients with acute MI show highest TN-C serum levels on Day 5,[9] and peak TN-C levels are predictive for severe cardiac adverse events.[10] However, there is growing evidence that up-regulation of myocardial and circulating TN-C is associated with adverse LV remodelling; nevertheless, the underlying mechanisms are still fairly unknown. Our previous study[7] suggested the potential interaction between TN-C and angiotensin II (Ang-II). Fibrosis and heart failure following MI are stimulated by activation of the renin–angiotensin system (RAAS). Thereby, via up-regulation of angiotensin-converting enzyme (ACE), Ang-II induces fibrotic remodelling and cardiac hypertrophy.[11,12] A recent study from our group revealed that hypoxia and hypertrophic stimuli induce an increase of TN-C in H9c2 cells.[7] Furthermore, TN-C regulates MMPs and integrins in progression of LV hypertrophy as well as induces BNP and Ang-II up-regulation.[7] The purpose of this experimental study was to elucidate haemodynamic effects of TN-C as well as changes in ECM remodelling and the RAAS system after MI in a TN-C KO model. To our knowledge, this is the first experimental study in infarcted KO mice, which describes the effects of TN-C using magnetic resonance imaging (MRI) and the isolated working heart and provides a molecular explanation for the haemodynamic findings.

Methods

Myocardial infarction model

Male TN-C KO mice (KO, RBRC00007 A, Experimental Animal Division, Tsukuba, Japan)[13–15] and their wild-type littermates (WT, A/J, #000646, The Jackson Laboratory, Sacramento, CA, USA) underwent MI or sham operation (WT-sham: n = 20; KO-sham: n = 20; WT-MI: n = 32; and KO-MI: n = 36). As described recently,[16] left lateral thoracotomy was performed under deep isoflurane anaesthesia. The pericardium was opened, and the left coronary artery exposed and surely ligated below the left atrial auricle with a 6.0 polyethylene suture. Transmural MI was confirmed by immediate myocardial paling below the suture and ST-segment elevation in the electrocardiogram. Afterwards, the chest was closed with single sutures. Animals were extubated, when spontaneous breathing was observed. Sham animals underwent the same procedure without coronary artery occlusion. Buprenorphine was used as pain medication pre-operatively and post-operatively (0.1 mg/kg, i.p.). Mice received food and water *ad libitum*. Euthanasia was performed with ketamine (100 mg/kg, i.p.) and xylazine (12 mg/kg, i.p.). All experiments were approved by the Ethics Committee for Laboratory Animal Research of the Medical University of Vienna (GZ: 66.009/0173-II/10b/2009). The investigation conforms to the Guide for the Care and Use of Laboratory Animals published by the US National Institutes of Health (NIH Publication No. 85-23, revised 1985).

Cardiac magnetic resonance imaging

Six weeks after MI, mice were anaesthesized with isoflurane 1.5% via a respiration cone and MRI was performed under spontaneous breathing and steady control of vital parameters on Medspec 3T MR system (Bruker, BioSpin, Rheinstetten, Germany). For assessment of the LV function, Segment—Software for Quantitative Medical Image Analysis (v1.8 R1172, Medviso AB, Lund, Sweden) was used. Edges of LV endocard and epicard were traced with inclusion of papillary muscle in the multi-slice short axes images. The following parameters were quantified: LV end-systolic volume, LV end-diastolic volume (LVEDV), ejection fraction (EF), and fractional shortening.[15]

Haemodynamics

Ex vivo haemodynamic evaluation analysis was performed with the isolated working heart (IH-1/IH-SR, Hugo Sachs, March-Hugstetten, Germany), as described recently.[15] All data were recorded with Labchart (v7.3.2) on a Powerlab System (8/30, both AD Instruments, Spechbach, Germany).[17] The following parameters were measured: heart rate, electrocardiogram, aortic pressure, LV pressure (LVP), aortic flow, left atrial flow, and coronary flow. For the measurement of LVP, a Mikro-Tip catheter (SPR-1000, Millar Instruments, Houston, TX, USA) was inserted retrogradely via the aortic valve. External heart work was calculated by cardiac output × systolic LVP for each time point. Systolic and diastolic wall stress were calculated accordingly: LVP × LV radius/(2× wall thickness) as recently published.[16]

Organ preparation

One and six weeks after surgery, beating hearts were excised under deep anaesthesia and instantly dissected for biochemical assay hearts. Three samples of the septum were taken and snap frozen in liquid nitrogen and stored at −80°C for PCR analyses. For immunohistochemistry (IHC), hearts were immersed in 10% buffered formaldehyde immediately after excision. After 48 h, hearts were cut at mid-papillary level and embedded in paraffin. Sections of 4 μm were stained with Goldner trichrome and Picrosirius Red for histopathological analyses or with antibodies for protein semi-quantification. For infarct size, quantification after Goldner trichrome staining length measurement was applied as previously described.[18]

Picrosirius Red staining

For histological fibrosis quantification, the samples were transversally cut on a mid-papillary level, fixed with formalin, and embedded in paraffin followed by staining according to the manufacturer's instructions (Picrosirius Red Kit, Polysciences Inc., Warrington, FL, USA). The colour threshold tool of ImageJ (NIH, Bethesda, MD, USA) was used to quantify the amount of fibrosis of the remote area.

Masson–Goldner trichrome stain

A Masson–Goldner trichrome kit (Carl Roth GmbH, Karlsruhe, Germany) was utilized to quantify fibrous connective tissue, which turns blue after staining and represents the myocardial scar. Therefore, microscope slides (MSs) were treated in xylol (3 min) and ethanol 100%, 96%, and 70% (3 min each) and subsequently washed in demineralized water (DI) before hemalm staining for 1 min and blueing for 5 min. The slides were then stained with all three Goldner solutions (I: 1 and 5 min; II: 2 min; and III: 5 min), rehydrated, and covered with Aquatex (Merck Millipore, Darmstadt, Germany).

Immunohistochemistry

For IHC, we established primary anti-mouse antibodies for MMP-9 (1:200, C-20, sc-6840), TIMP-1 (1:100, H-150, sc-5538), and TIMP-3 (1:200, bs-0417R, Bioss Inc., Woburn, MA, USA). The staining protocol was as follows: MSs were primarily deparaffinized in xylol (20 min) and ethanol 100%, 96%, and 70% (10 min each). Afterwards, MSs were washed in DI for 2 min, stored in citrate buffer for another 5 min, cooked in a microwave oven for 20 min, and finally cooled at room temperature for another 45 min. Subsequently, a protein block (Protein Block Serum Free, X0909, Dako, Vienna, Austria) was applied, and slides were stored in the fridge at 4°C for 60 min. Meanwhile, primary antibodies were diluted (Antibody Diluent, S3022, Dako) at pretested concentrations. Then, around 50 μL of diluted primary antibody was dropped on each slide, and the MSs were put back into the fridge at 4°C overnight. Pure antibody diluent was applied on negative controls. On the next day, MSs were washed in Tris (Tris-buffered saline, Sigma-Aldrich, Steinheim, Germany) two times for 5 and 20 min at 4°C. After application of the secondary antibody, MSs were incubated for 20 min at 37°C followed by another wash cycle in Tris buffer for 10 min. Subsequently, streptavidin peroxidase (HK 330 9K, Biogenex, Fremont, CA, USA) was dropped on MS and stored for another 20 min at 37°C. Then, MSs were stained with DAB (Peroxidase Substrate Kit DAB, SK-4100, Dako) for 3 min and washed in DI water for 5 min, counterstained with hemalm for 3 min, blued for 5 min, and covered with Aquatex (Merck Millipore). Immunostaining semi-quantification was performed with ImageJ software.[19] The immunoreactive proportion of the total remote surface area was described in per cent.[20]

Real-time PCR

Myocardial samples from the ventricular septum (remote area of MI) were analysed with real-time PCR. RNA levels of MMP-9, TIMP-1, and TIMP-3 were quantified. All levels were adjusted for GAPDH. mRNA was purified using High Pure Tissue RNA Isolation Kit (Roche, Basel, Switzerland) according to the instruction manual. Transcription into cDNA was performed with a Transcriptor First Strand cDNA Synthesis Kit (Roche).

For real-time PCR, a LightCycler® TaqMan® Master Universal ProbeLibrary (Roche) was used. Primers were designed on the basis of the Roche Universal ProbeLibrary Assay Design Center (http://www.universalprobelibrary.com/).

Serum angiotensin-converting enzyme activity

One week after MI, serum ACE activity was measured with an artificial fluorescent substrate (Abz-FRK(Dnp)P; Enzo Life Sciences, Farmingdale, New York, USA) in a reaction mixture containing 100 mM Tris–HCl (Tris(hydroxymethyl) aminomethane hydrochloride), 15 μM Abz-FRK(Dnp)P, 50 mM NaCl, 10 μM $ZnCl_2$, and serum samples, at pH 7.0. Serum samples were diluted 100-fold in order to eliminate the endogenous ACE inhibition mediated by albumin.[21] Measurements were performed in 96-well black plates (Greiner Bio-One, Kremsmuenster, Austria) at 37°C. Changes in fluorescence intensity (excitation: 340 nm; emission: 420 nm) were measured at 30 s intervals for at least 15 min with a plate reader (NOVOstar plate reader; BMG Labtech, Ortenberg, Germany). Fluorescence intensity values were plotted as a function of reaction time and fitted by linear regression.

The fit and the data were accepted when r^2 was 0.95. ACE activity was calculated via the equation: ACE activity (U/L) = $S/k * D$, where S is the rate of observed increase in fluorescence intensity (1/min), k is the change in fluorescence intensity upon the complete cleavage of 1 μmol of Abz-FRK(Dnp)P, and D is the dilution of the serum.[21]

Serum angiotensin-converting enzyme concentration

Serum ACE concentration was measured by a commercial mouse ACE ELISA development kit (Cat No. DY1513, R&D Systems, Minneapolis, Minnesota, USA) according to the manufacturer's instructions with minor modifications. Enzyme-linked immunosorbent plates (Sigma-Aldrich) were coated with 400 ng per well capture antibody. The remaining binding sites were then blocked with reagent diluent [10 mg/mL bovine serum albumin (Sigma-Aldrich, St. Louis, Missouri, USA) in Dulbecco's phosphate buffered saline solution (Gibco, Thermo Fisher Scientific, Waltham, Massachusetts, USA)]. Diluted sera (in reagent diluent, 100-fold dilution) were added to the wells, and the antibody–antigen complexes were labelled with a biotinylated detection antibody (40 ng per well); 200-fold-diluted streptavidin–horseradish peroxidase conjugate (kit component) was added to the wells. Finally, the amounts of complexes were detected with a substrate solution containing 0.3 mg/mL tetramethylbenzidine, 0.1 mM H_2O_2, and 50 mM acetic acid. The reaction was terminated after 20 min by the addition of 0.5 M HCl, and the optical density was measured at 450 nm.[21]

Myocardial angiotensin-converting enzyme concentration and activity

Myocardial samples from the border zone of infarction as well as remote zone (septum) were analysed 1 week after MI. Frozen tissue samples were homogenized in ACE diluting buffer [100 mM Tris–HCl (Tris(hydroxymethyl)aminomethane hydrochloride) containing 50 mM NaCl, 10 μM $ZnCl_2$, and 0.6% Triton X-100, pH 7.0] in 0.1 mg wet tissue/mL concentration. The homogenates were centrifuged (16 000 *g* for 10 min), and the supernatants were used for the biochemical determinations. The protein content was determined by bicinchoninic acid assay and adjusted to 1 mg/mL with the Tris buffer mentioned earlier. This supernatant was measured at 20-fold dilution. The reaction mixture contained 10 μL tissue sample (adjusted to 1 mg/mL), 90 μL ACE diluting buffer (see aforementioned), and 100 μL of substrate solution (30 μM Abz-FRK(Dnp)P in ACE diluting buffer). The reaction took place by the addition of the substrate. The fluorescence intensities were recorded by a NOVOstar plate reader (BMG Labtech; excitation: 340 nm; emission: 420 nm) at 37°C, and the activities were calculated as described for the measurement of serum ACE activity. The activities were normalized to the measured protein contents to yield ACE activity in absolute units.

Statistical analyses

Statistical testing was performed with GraphPad Prism (7.0d, GraphPad Software, La Jolla, CA, USA). Haemodynamic variables were compared with two-way ANOVA for repeated measurements with Sidak *post hoc* test for multiple comparisons. Binary events were compared with Fisher's exact test. Metric values were presented as absolute values or as mean ± standard deviation. A P-value of <0.05 was considered significant.

Results

Animal characteristics

Values are depicted in *Table 1*. In total, 36 TN-C KO mice were infarcted. Out of those, 14 mice died (39%) within the first 48 h. The surviving mice were divided in one group, sacrificed after 1 week (n = 8) and 6 weeks (n = 8) for IHC and biochemistry, and the other group, sacrificed after 6 weeks after MI (n = 6) for MRI and isolated working heart analysis. For WT control group, 32 WT mice were infarcted. Out of those, eight mice died (25%) within the first 48 h. The surviving mice were also divided in one group, sacrificed after 1 week (n = 8) and 6 weeks (n = 8), only for IHC and biochemistry, and the other group, sacrificed after 6 weeks after MI (n = 8) for haemodynamic measurements. In addition, sham operations were performed (WT: n = 20; KO: n = 20), and all animals survived until sacrifice.

Six weeks after MI, mean infarction size was similar in both strains (WT-MI: 49 ± 9 and KO-MI: 57 ± 3%, n.s.; Supporting Information, *Figure S1*). Total heart weight (THW) was significantly higher in MI than in sham groups (WT: 219.4 ± 28.8 vs. 157.2 ± 7.1 mg; KO: 201.5 ± 43.4 vs. 141.0 ± 10.6 mg; both $P < 0.01$), while THW was comparable between strains. The total heart weight to body weight ratio (THW/BW) was increased in MI vs. sham groups. (WT: 8.2 ± 0.9 vs. 6.5 ± 0.6 mg/g; $P < 0.01$). However, in TN-C KO mice, this effect was below significance (TN-C KO-MI vs. TN-C KO-sham: 6.5 ± 0.6 vs. 5.6 ± 0.3 mg/g; n.s.). The difference in THW/BW ratio between WT-MI and TN-C KO-MI was likewise significant (8.2 ± 0.9 vs. 6.5 ± 0.6 mg/g; $P < 0.05$), indicating less hypertrophy in TN-C KO-MI mice. Picrosirius Red staining of the remote zone showed an analogous picture as THW/BW ratio. WT-MI had significantly higher collagen levels when compared with TN-C KO-MI (8.1 ± 1.5% vs. 3.6 ± 0.5%; $P < 0.01$), indicating more fibrosis.

Table 1 Animal characteristics and haemodynamic magnetic resonance imaging results of sham and MI groups 6 weeks after operation

Parameter	WT-SH (n = 8)	TN-C KO-SH (n = 7)	P	WT-MI (n = 8)	TN-C KO-MI (n = 6)	P
BW (g)	25.32 ± 2.34	23.41 ± 3.20**	0.02	26.56 ± 1.80	26.65 ± 2.64**	0.86
THW (mg)	157.2 ± 7.1**	141.0 ± 10.6**	0.001	219.4 ± 28.8**	201.5 ± 43.4**	0.25
THW/BW (mg/g)	6.6 ± 0.5**	5.6 ± 0.3**	0.93	8.2 ± 0.9**	6.5 ± 0.6**	0.02
Tibia (mm)	18.48 ± 7.6	18.97 ± 0.83	0.29	18.94 ± 1.22	18.53 ± 1.39	0.66
LU wdr	4.48 ± 0.52	4.37 ± 0.28**	0.65	4.67 ± 0.43	5.64 ± 0.72**	0.004
LI wdr	3.05 ± 0.12	3.11 ± 0.10	0.36	3.20 ± 0.13	2.93 ± 0.35	0.58
Infarct size (%)	0	0	1	49 ± 9	57 ± 3	0.20
Post-MI mortality (%)	0 (0)	0 (0)	1	8 (25)	14 (39)	0.30
Col (%)	1.3 ± 0.2**	3.6 ± 0.4		8.1 ± 1.5**	3.6 ± 0.5	
HR (b.p.m.)	489 ± 49	478 ± 27	0.50	480 ± 49	496 ± 42	0.17
LVEDV (μL/g)	236 ± 38**	228 ± 40	0.72	514 ± 150**	341 ± 111	0.009
LVESV (μL/g)	75 ± 25**	73 ± 16**	0.87	484 ± 176**	282 ± 54**	0.003
EF (%)	67 ± 8**	69 ± 4**	0.43	26 ± 6**	24 ± 7**	0.61
FS (%)	46 ± 10**	49 ± 4**	0.88	16 ± 4**	19 ± 8**	0.54
LVEDP (mmHg)	6 ± 1.6	6 ± 1.7	0.99	8.4 ± 1.4	5.8 ± 1.8	0.02
Systolic wall stress	37.7 ± 11.6**	31.1 ± 10.2**	0.34	67.3 ± 14.1**	47.5 ± 7.4**	0.01
Diastolic wall stress	6.5 ± 3.0*	4.7 ± 1.2*	0.25	11.2 ± 2.0*	8.2 ± 2.5*	0.03

BW, body weight; Col, collagen ratio; EF, ejection fraction; FS, fractional shortening; HR, heart rate; LI wdr, wet/dry liver weight ratio; LU wdr, wet/dry lung weight ratio; LVEDP, left ventricular end-diastolic pressure; LVEDV, left ventricular end-diastolic volume; LVESV, left ventricular end-systolic volume; MI, myocardial infarction; THW, total heart weight; THW/BW, total heart weight to body weight ratio; Tibia, tibia length. All values in mean ± standard deviation.
*P < 0.05 indicates differences between MI and sham groups of same strain.
**P < 0.01 indicates differences between MI and sham groups of same strain.

Cardiac magnetic resonance imaging

Data are depicted in *Table 1*. LVEDV was significantly increased in WT-MI vs. WT-sham (514 ± 150 vs. 236 ± 38 μL/g; P < 0.01). In contrast, in TN-C KO-MI vs. TN-C KO-sham, no significant difference was observed (341 ± 111 vs. 228 ± 40 μL/g; n.s.). Nonetheless, TN-C KO-MI showed significantly lower LVEDV compared with WT-MI (341 ± 111 vs. 514 ± 150 μL/g; P < 0.01), indicating less diastolic ventricular dilation. LV end-systolic volume was significantly increased in WT-MI vs. WT-sham (484 ± 176 vs. 75 ± 25 μL/g; P < 0.01) as well as TN-C KO-MI vs. TN-C KO-sham (282 ± 54 vs. 73 ± 16 μL/g; P < 0.01). In TN-C KO-MI vs. WT-MI, a significantly decreased LV end-systolic volume was observed (282 ± 54 vs. 484 ± 176 μL/g; P < 0.01), also indicating less systolic ventricular dilation in TN-C KO. EF was significantly decreased in WT-MI vs. WT-sham (26 ± 6% vs. 67 ± 8%; P < 0.01) and TN-C KO-MI vs. TN-C KO-sham (24 ± 7% vs. 69 ± 4%; P < 0.01); however, EF was comparable in TN-C KO-MI vs. WT-MI: 24 ± 7% vs. 26 ± 6%; n.s.; Supporting Information, *Figure S2*).

Isolated working heart–*ex vivo* haemodynamic data

Data are depicted in *Tables 1* and *2* and *Figure 1*. Characterization on the isolated heart was successfully performed in eight WT-sham, seven TN-C KO-sham, eight WT-MI, and six TN-C KO-MI mice. Flow values were normalized to heart weight. Cardiac output (*Figure 1A*), stroke volume (*Figure 1B*), external heart work (*Figure 1C*), and aortic flow (*Figure 1D*) were significantly (P < 0.05) higher in TN-C KO-MI when compared with WT-MI. Coronary flow was significantly lower during the entire observation period in MI hearts, independent of the strain (both P < 0.01). LVEDP was significantly decreased in TN-C KO-MI vs. WT-MI at 20 min of working heart experiments (8.4 ± 1.4 vs. 5.8 ± 1.8 mmHg; P < 0.05; *Table 1*).

Wall stress (∂⁄, *Table 1*) was calculated at time point 20 min in working heart mode. While sham animals of both strains were similar (WT vs. TN-C KO: ∂⁄systolic: 32.6 ± 6.6 vs. 28.4 ± 7.4 mmHg; ∂⁄diastolic: 13.0 ± 6.0 vs. 9.4 ± 2.4 mmHg; both n.s.), TN-C KO-MI showed significantly lower systolic (47.5 ± 7.4 vs. 67.3 ± 14.1 mmHg; P < 0.01) and end-diastolic ∂⁄(7.4 ± 2.0 vs. 11.2 ± 2.0 mmHg; P < 0.01) than WT-MI.

Reverse transcription polymerase chain reaction and immunohistochemistry from remote area

Values are depicted in *Figure 2* and Supporting Information, *Figures S3* and *S4*.

One week after MI, TN-C mRNA expression was significantly decreased in TN-C KO-MI vs. WT-MI (1.95 ± 0.79 vs. 45.14 ± 11.81; P < 0.0001); after 6 weeks, there was still a tendency for lower TN-C mRNA in TN-C KO-MI (1.47 ± 0.47 vs. 6.25 ± 3.41; P = 0.74). One week after MI, mRNA levels of MMP-9 were similar in all groups. Six weeks after MI, mRNA levels of MMP-9 were significantly decreased in TN-C KO-MI vs. WT-MI (1.21 ± 0.14 vs. 2.39 ± 0.34; P < 0.01; *Figure 2*). Protein expression showed a similar pattern to mRNA levels (TN-C KO-MI vs. WT-MI: 2.4 ± 0.1% vs. 6.2 ± 0.2%;

Table 2 Haemodynamic measurements during working heart mode

Index	Group	Time points							
		5′	10′	15′	20′	25′	Pw	Pg	Pi
Systolic AP (mmHg)	WT-MI	67 ± 5	68 ± 5	68 ± 4	67 ± 3	67 ± 3	0.152	0.752	0.862
	TN-C KO-MI	65 ± 5	66 ± 4	66 ± 4	65 ± 6	64 ± 7			
Systolic LVP (mmHg)	WT-MI	76 ± 9	79 ± 10	79 ± 10	79 ± 9	74 ± 7	0.083	0.735	0.294
	TN-C KO-MI	74 ± 6	75 ± 7	77 ± 5	74 ± 7	75 ± 6			
Aortic flow (mL/g HW)	WT-MI	8.5 ± 3.8	8.5 ± 3.8	8.4 ± 4.6	7.9 ± 4.0	7.4 ± 3.4	0.455	0.025	0.904
	TN-C KO-MI	11.7 ± 5.8	12.2 ± 5.6	12.6 ± 5.5	12.1 ± 5.8	11.3 ± 5.5			
Coronary flow (mL/g HW)	WT-MI	10.1 ± 2.5	9.9 ± 2.1	8.9 ± 2.1	7.8 ± 3.4	7.6 ± 3.8	0.003	0.365	0.148
	TN-C KO-MI	7.9 ± 2.5	7.8 ± 2.4	8.2 ± 2.6	7.4 ± 3.0	6.8 ± 3.0			
CO (mL/g HW)	WT-MI	18.4 ± 5.5	19.2 ± 5.6	18.5 ± 6.3*	16.9 ± 7.2	15.8 ± 6.5*	0.015	0.016	0.991
	TN-C KO-MI	21.8 ± 8.5	22.6 ± 8.5	22.6 ± 7.9*	21.4 ± 8.4	20.8 ± 8.4*			
Stroke volume (μL/g HW)	WT-MI	50.7 ± 17.9	53.1 ± 14.4	51.9 ± 15.7	46.5 ± 15.8*	46.0 ± 18.1*	0.662	0.018	0.775
	TN-C KO-MI	73.4 ± 19.8	75.0 ± 21.1	75.7 ± 21.5	74.9 ± 25.0*	74.3 ± 25.5*			
Exernal heart work (CO × LVP)	WT-MI	1286 ± 505	1411 ± 591	1338 ± 657	1224 ± 708	1004 ± 470*	0.207	0.021	0.951
	TN-C KO-MI	2227 ± 512	2339 ± 633	2255 ± 667	2181 ± 741	2113 ± 737*			

AP, arterial pressure; CO, cardiac output; HW, heart weight; LVP, left ventricular pressure.
Data are given as mean ± standard deviation; *P*-values are given for within groups (Pw; time), between groups (Pg), and interaction (Pi) from two-way repeated measures ANOVA. *Post hoc* analysis was performed with Sidak test.
*$P < 0.05$.

$P < 0.001$; Supporting Information, *Figure S3*). One week after infarction, mRNA levels of TIMP-1 were significantly increased in MI hearts of both strains when compared with sham. However, TIMP-1 mRNA levels were significantly lower in TN-C KO-MI than in WT-MI (6.26 ± 0.60 vs. 10.49 ± 1.31; $P < 0.01$; *Figure 2*). This difference remained significant also for 6 weeks after MI (1.99 ± 0.31 vs. 4.70 ± 0.75; $P < 0.01$; *Figure 2*). IHC results were comparable to mRNA (1 week: 1.02 ± 0.06% vs. 3.39 ± 0.18%; 6 weeks: 1.34 ± 0.12% vs. 2.18 ± 0.24%; Supporting Information, *Figure S3*). One week after infarction, mRNA levels of TIMP-3 were significantly higher in TN-C KO-MI than in WT-MI (1.07 ± 0.08 vs. 0.60 ± 0.04; $P < 0.001$; *Figure 2*). Six weeks after MI, there was no difference between strains. IHC results were comparable to mRNA (1 week: 3.61 ± 0.48 vs. 2.23 ± 0.22; $P < 0.05$; Supporting Information, *Figure S3*). The TIMP-3/MMP-9 ratio between TN-C KO-MI and WT-MI was significantly elevated 1 week (1.04 ± 0.15 vs. 0.41 ± 0.02; $P < 0.01$; *Figure 2*) and 6 weeks after infarction (1.44 ± 0.19 vs. 0.65 ± 0.12; $P < 0.01$; *Figure 2*).

Figure 1 Cardiac output (mL/min/g heart weight, A), stroke volume (μL/beat/g wet heart weight, B), external heart work (CO × LVP, C), aortic flow (mL/min/g heart weight, D), WT-MI wild-type MI (red), and KO-MI tenascin-C knockout MI (blue). Data are given as mean ± standard deviation; *P*-values are given for within groups (Pw; time), between groups (Pg), and interaction (Pi) from two-way repeated measures ANOVA. *Post hoc* analysis was performed with Sidak test: *$P < 0.05$.

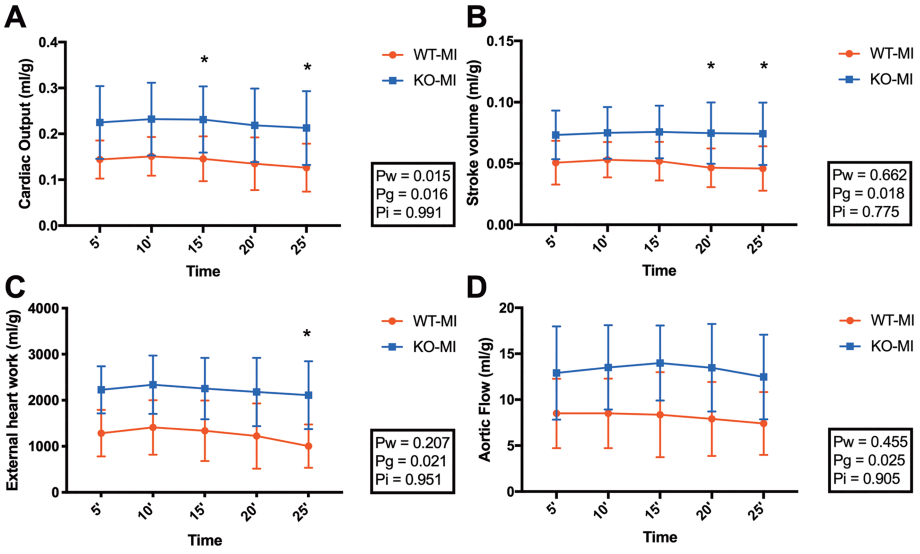

Figure 2 Remote zone mRNA levels (1/GAPDH) of MMP-9, TIMP-1, and TIMP-3, TIMP-3/MMP-9 ratio, and TN-C WT-MI (red) and TN-C KO-MI (blue) 1 and 6 weeks after infarction; $^{*}P < 0.05$, $^{**}P < 0.01$, and $^{***}P < 0.001$.

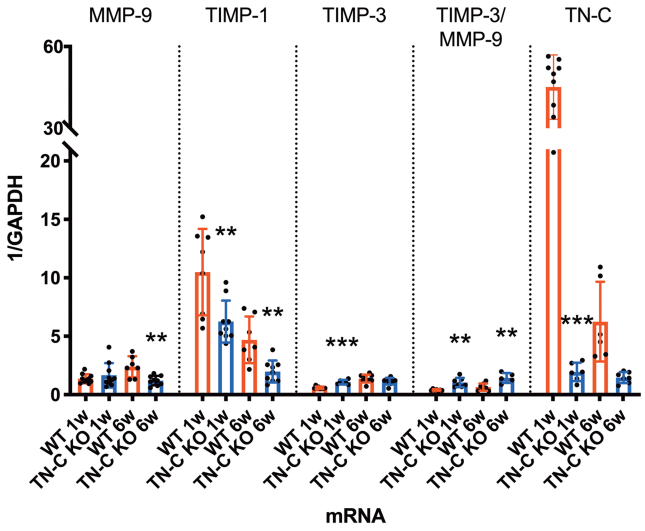

Angiotensin-converting enzyme concentration and activity

One week after MI, myocardial ACE activity in the border zone was significantly lower in TN-C KO than in WT (627.5 ± 155.3 vs. 889.2 ± 139.9 U/L; $P < 0.01$; *Figure 3A*). There was a tendency for reduction of ACE activity in the remote zone as well (TN-C KO-MI 419.0 ± 159.6 vs. WT-MI 555.3 ± 159.0 U/L; $P = 0.41$; *Figure 3A*). In contrast, circulating ACE concentration (900.9 ± 166.1 vs. 564.4 ± 83.31 µg/L; $P < 0.0001$; *Figure 3B*) and ACE activity (33.0 ± 4.9 vs. 25.6 ± 3.4 U/L; $P < 0.0037$; *Figure 3C*) were significantly higher in TN-C KO-MI than in

Figure 3 (A) Myocardial angiotensin-converting enzyme (ACE) activity was significantly reduced in the border zone in TN-C KO (TN-C) vs. WT mice 1 week after myocardial infarction (MI). In addition, there was a tendency for a complementary reduction in the remote zone as well but without significance. Circulating ACE (B) and activity (C) were significantly increased in TN-C KO 1 week after MI. (D) ACE2 activity was unaffected in TN-C KO 1 week after MI.

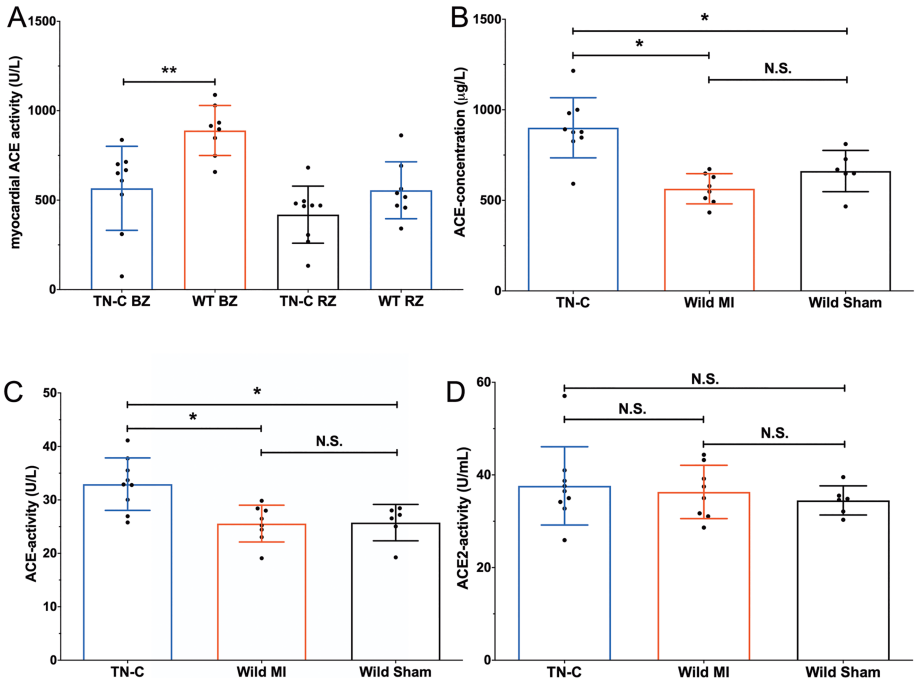

WT-MI 1 week after MI. In addition, ACE concentration (564.4 ± 83.3 vs. 661.9 ± 114.0 U/L; n.s.; *Figure 3B*) and ACE activity (25.6 ± 3.4 vs. 25.8 ± 3.4 U/L; $P = 0.996$; *Figure 3C*) were similar in WT-MI and WT-sham. ACE2 activity did not show a difference between the groups (*Figure 3D*).

Discussion

In a TN-C KO-MI model, for the first time, we show that TN-C aggravates LV dilatation with concomitant fibrosis and up-regulation of ACE activity within MI. Consecutively, lack of TN-C resulted in preserved LV haemodynamics as shown by MRI and in the isolated heart.

Six weeks after MI, we describe reduced LVESD and LVEDD in TN-C KO-MI, while EF and fractional shortening are similar to WT-MI. These results are in line with existing literature[22] as well as our previous study, where we reported TN-C KO mice with significantly reduced LVEDD compared with WT in a mouse model of chronic pressure overload.[6] Additionally, in patients with dilated cardiomyopathy, myocardial expression of TN-C is increased and associated with worse long-term outcome.[23]

Because EF was similar between the two infarcted groups, we aimed to investigate LV function in an isolated working heart model. Then, we combined *in vivo* and *ex vivo* data, to describe systolic and end-diastolic wall stress, thereby generating load control and EF-independent parameters.[24] Accordingly, TN-C KO-MI showed a significant reduction in both systolic and end-diastolic wall stress, suggesting a decrease in myocardial oxygen demand. In addition, increased wall stress is a sign for attenuated sarcomere shortening and, subsequently, less SV and dilatation.[25]

In addition, there is substantial evidence that the ECM remodelling represents the pathological substrate of LV dilatation following MI.[26] Therefore, we assessed the expression patterns of TIMPs and MMPs in the remote zone of TN-C KO and WT mice after MI. Furthermore, we aimed to link TN-C with relevant ECM proteins TIMP-1, TIMP-3, and MMP-9. For the first time, we showed that lack of TN-C resulted in TIMP-1 mRNA down-regulation and that reduced TIMP-1 expression does not necessarily mean worse remodelling as shown in our TN-C KO mice. TIMP-1 has a regulatory effect on MMPs. In healthy hearts, the lack of TIMP-1 results in greater LVEDV and end-diastolic wall stress as well as a decrease in collagen content, while systolic LVP and EF stay unchanged. Our results suggest that the extent of the TIMP-1 increase after MI might not be as important as the increase itself.[27,28] After MI, LVEDV and LV end-diastolic pressure are increased in TIMP-1-KO mice, which also show signs of progressed hypertrophy.[29]

Next to TIMP-1, TIMP-3 seems to be down-regulated by TN-C after MI; therefore, TN-C might regulate TIMP-3 expression after MI. Instead of increased fibrosis, TN-C KO presented with attenuated amounts of collagen with the lack of increased cardiac rupture. This is in line with data from infarcted TIMP-3 KOs that showed reduced collagen, greater LV dilatation, increased mortality rates, and higher MMP-2/MMP-9 activity.[30] Additionally, in ischaemic and dilated human cardiomyopathy, TIMP-1 and TIMP-3 are significantly down-regulated in LV myocardium, while MMP-9 is highly elevated.[31] In our study, 6 weeks after MI, MMP-9 was significantly down-regulated in TN-C KO. Together with reduced LV dilatation, our data are confirmed by results from MMP-9 KO mice, which had reduced LV end-diastolic and end-systolic diameters following MI.[32]

Recently, our group showed that H9c2 cardiomyoblasts exposed to TN-C significantly increased mRNA levels of MMP-9.[7] In line with that, myocardial interstitial fibrosis was reduced in TN-C KO mice following chronic pressure overload stimulation, and significant increase in the expression of ANP and BNP mRNA levels was observed in H9c2 cells after the administration of recombinant human TN-C incubation.[6]

Recently, we found that Ang-II regulates TN-C in epigenetic levels; however, their interaction has not been fully understood.[7] Of importance, the pharmacological inhibition of ACE has beneficial effects on post-MI remodelling, including reduction in fibrosis, LV dilatation, and apoptosis.[33] ACE and Ang-II are produced from both the infarcted/perinfarct and remote myocardia by predominantly endothelial cells and macrophages in the early phase and later by myofibroblasts in the infarcted and border zone.[34–38] The consequent release of Ang-II mediates hypertrophy, apoptosis, and fibrosis, all of which are contributors to adverse LV remodelling. Accordingly, our results demonstrated the local up-regulation of ACE (mainly in the border zone) following MI. In contrast, TN-C KO mice showed a significant reduction in ACE activity in the border zone in association with less amount of fibrosis and remodelling. In addition, there is evidence that ACE up-regulation results in LV dysfunction and expression and activity of MMPs as well as TIMPs, which are contributors of adverse post-MI remodelling.[39] Interestingly, the circulating concentration of ACE and activity was higher in TN-C KO after 1 week after MI; the latter finding needs to be clarified in future studies.

Our data do not provide evidence for the underlying mechanism of TN-C in up-regulation of ACE expression or activity; however, we strongly believe that TN-C enhances ACE activity and, subsequently, LV dilatation and haemodynamic dysfunction after MI.

Limitations

This experimental study has the following limitations: blood pressure was only measured *ex vivo*; nevertheless, we could show that *in vivo* and *ex vivo* haemodynamic parameters

correlate in mice after MI.[16] We observed higher post-MI mortality in TN-C KO, which is explained by the low number of used animals; we cannot report of a higher susceptibility for acute MI in these mice. Another limitation to our study is the lack of MMP-2 data, which were technically impossible because of small amount of available tissue material. In order to follow the principles of the 3Rs, we decided not to repeat the experiments for further analyses.

In 2010, Nishioka *et al*.[22] described reduced fibrosis and improved post-MI remodelling in TN-C KO with echocardiography and histology. Our study takes the results of Nishioka and Gonçalves *et al*.[7] to the next level by confirmation with detailed haemodynamic analysis (MRI and isolated working heart) as well as by molecular description of ECM proteins in an *in vivo* model.

In conclusion, in this TN-C KO model, we show for the first time that TN-C is involved in post-MI LV dilatation and, thereby, might influence the ECM and RAAS pathways. The functional improvement of TN-C KO mice as described in the isolated working heart suggests that TN-C might qualify as a potential biochemical target for timed interventions.

Acknowledgements

Special thanks go to the Center for Biomedical Research, technician Milat Inci for enduring support during the project, and Mark Aronovitz (Tufts Medical Center, Boston, USA) who gave essential advice for the establishment of the MI model. We thank Ms Shalett Mathew (Center for Biomedical Research, Medical University of Vienna, Austria) for diligent proofreading of this manuscript.

Conflict of interest

None declared.

Funding

This work was supported by a continuous grant from the Ludwig Boltzmann Institute for Cardiovascular Research, Ludwig Boltzmann Gesellschaft, 1090 Vienna, Austria (Grant Number REM 2012-16); the Medical University of Vienna (Medizinische Universität Wien; grant Dissertationsstipendium); and the City of Vienna (MA 7) (Magistrat der Stadt Wien; Grant Number 2451/10).

Supporting information

Additional supporting information may be found online in the Supporting Information section at the end of the article.

Figure S1. Representative histological images of infarcted mouse hearts (WT: A, C, E; TN-C KO: B, D, F) after Goldner Trichrome (A, B) and Picro-Sirius-Red Staining (C, D, E, F). Images E and F are taken from the myocardial septum.
Figure S2. Representative MRI images of an infarcted mouse heart. The red line marks the LV volume. Edges of LV endocard were traced with inclusion of papillary muscle in the multi-slice short axes images.
Figure S3. Representatitve IHC images, bars: 100μm. MMP-9: A-D, TIMP-1: E-H, TIMP-3: I-L, AT: M-P,: WT-MI-1W (A, E, I, M); TN-C KO-MI-1W (B, F, J, N); WT-MI-6W (C, G, K, O); TN-C KO-MI-6W (D, H, L, P)
Figure S4. Immunoreactive proportion of the total remote surface area (%) of MMP-9, TIMP-1 and TIMP-3 in WT-MI (red) and KO-MI (blue) myocardial free wall 1 and 6 weeks after infarction; **P*<0.05, ***P*<0.01, ****P*<0.001.

References

1. Opie LH, Commerford PJ, Gersh BJ, Pfeffer MA. Controversies in ventricular remodelling. *Lancet*. [Review] 2006 Jan 28; **367**: 356–367.
2. Tamura A, Kusachi S, Nogami K, Yamanishi A, Kajikawa Y, Hirohata S, Tsuji T. Tenascin expression in endomyocardial biopsy specimens in patients with dilated cardiomyopathy: distribution along margin of fibrotic lesions. *Heart* 1996; **75**: 291–294.
3. Willems IE, Arends JW, Daemen MJ. Tenascin and fibronectin expression in healing human myocardial scars. *J Pathol* 1996; **179**: 321–325.
4. Morimoto S, Imanaka-Yoshida K, Hiramitsu S, Kato S, Ohtsuki M, Uemura A, Kato Y, Nishikawa T, Toyozaki T, Hishida H, Yoshida T, Hiroe M. Diagnostic utility of tenascin-C for evaluation of the activity of human acute myocarditis. *J Pathol* 2005; **205**: 460–467.
5. Nagel F, Santer D, Stojkovic S, Kaun C, Schaefer AK, Krssak M, Abraham D, Bencsik P, Ferdinandy P, Kenyeres E, Szabados T, Wojta J, Trescher K, Kiss A, Podesser BK. The impact of age on cardiac function and extracellular matrix component expression in adverse post-infarction remodeling in mice. *Exp Gerontol* 2019; **119**: 193–202.
6. Podesser BK, Kreibich M, Dzilic E, Santer D, Forster L, Trojanek S, Abraham D, Krssak M, Klein KU, Tretter EV, Kaun C, Wojta J, Kapeller B, Goncalves IF, Trescher K, Kiss A. Tenascin-C promotes chronic pressure overload-induced cardiac dysfunction, hypertrophy and myocardial fibrosis. *J Hypertens* 2018; **36**: 847–856.

7. Goncalves IF, Acar E, Costantino S, Szabo PL, Hamza O, Tretter EV, Klein KU, Trojanek S, Abraham D, Paneni F, Hallstrom S, Kiss A, Podesser BK. Epigenetic modulation of tenascin C in the heart: implications on myocardial ischemia, hypertrophy and metabolism. *J Hypertens* 2019; **37**: 1861–1870.
8. Imanaka-Yoshida K, Hiroe M, Nishikawa T, Ishiyama S, Shimojo T, Ohta Y, Sakakura T, Yoshida T. Tenascin-C modulates adhesion of cardiomyocytes to extracellular matrix during tissue remodeling after myocardial infarction. *Lab Invest* 2001; **81**: 1015–1024.
9. Terasaki F, Okamoto H, Onishi K, Sato A, Shimomura H, Tsukada B, Imanaka-Yoshida K, Hiroe M, Yoshida T, Kitaura Y, Kitabatake A. Higher serum tenascin-C levels reflect the severity of heart failure, left ventricular dysfunction and remodeling in patients with dilated cardiomyopathy. *Circ J* 2007; **71**: 327–330.
10. Sato A, Aonuma K, Imanaka-Yoshida K, Yoshida T, Isobe M, Kawase D, Kinoshita N, Yazaki Y, Hiroe M. Serum tenascin-C might be a novel predictor of left ventricular remodeling and prognosis after acute myocardial infarction. *J Am Coll Cardiol* 2006; **47**: 2319–2325.
11. Ishiyama Y, Gallagher PE, Averill DB, Tallant EA, Brosnihan KB, Ferrario CM. Upregulation of angiotensin-converting enzyme 2 after myocardial infarction by blockade of angiotensin II receptors. *Hypertension* 2004; **43**: 970–976.
12. Xia QG, Chung O, Spitznagel H, Sandmann S, Illner S, Rossius B, Jahnichen G, Reinecke A, Gohlke P, Unger T. Effects of a novel angiotensin AT_1 receptor antagonist, HR720, on rats with myocardial infarction. *Eur J Pharmacol* 1999; **385**: 171–179.
13. Koyama Y, Kusubata M, Yoshiki A, Hiraiwa N, Ohashi T, Irie S, Kusakabe M. Effect of tenascin-C deficiency on chemically induced dermatitis in the mouse. *J Invest Dermatol* 1998; **111**: 930–935.
14. Matsuda A, Yoshiki A, Tagawa Y, Matsuda H, Kusakabe M. Corneal wound healing in tenascin knockout mouse. *Invest Ophthalmol Vis Sci* 1999; **40**: 1071–1080.
15. Nakao N, Hiraiwa N, Yoshiki A, Ike F, Kusakabe M. Tenascin-C promotes healing of Habu-snake venom-induced glomerulonephritis: studies in knockout congenic mice and in culture. *Am J Pathol* 1998; **152**: 1237–1245.
16. Santer D. *In vivo* and *ex vivo* functional characterization of left ventricular remodelling after myocardial infarction in mice. *ESC Heart Failure* 2015; **2**: 171–177.
17. Liao R, Podesser BK, Lim CC. The continuing evolution of the Langendorff and ejecting murine heart: new advances in cardiac phenotyping. *Am J Physiol Heart Circ Physiol* 2012; **303**: H156–H167.
18. Takagawa J, Zhang Y, Wong ML, Sievers RE, Kapasi NK, Wang Y, Yeghiazarians Y, Lee RJ, Grossman W, Springer ML. Myocardial infarct size measurement in the mouse chronic infarction model: comparison of area- and length-based approaches. *J Appl Physiol* 2007; **102**: 2104–2111.
19. Schneider CA, Rasband WS, Eliceiri KW. NIH Image to ImageJ: 25 years of image analysis. *Nat Methods* 2012; **9**: 671–675.
20. Heymans S, Lupu F, Terclavers S, Vanwetswinkel B, Herbert JM, Baker A, Collen D, Carmeliet P, Moons L. Loss or inhibition of uPA or MMP-9 attenuates LV remodeling and dysfunction after acute pressure overload in mice. *Am J Pathol* 2005; **166**: 15–25.
21. Fagyas M, Uri K, Siket IM, Darago A, Boczan J, Banyai E, Edes I, Papp Z, Toth A. New perspectives in the renin-angiotensin-aldosterone system (RAAS) I: endogenous angiotensin converting enzyme (ACE) inhibition. *PLoS ONE* 2014; **9**: e87843.
22. Nishioka T, Onishi K, Shimojo N, Nagano Y, Matsusaka H, Ikeuchi M, Ide T, Tsutsui H, Hiroe M, Yoshida T, Imanaka-Yoshida K. Tenascin-C may aggravate left ventricular remodeling and function after myocardial infarction in mice. *Am J Physiol Heart Circ Physiol* 2010; **298**: H1072–H1078.
23. Yokokawa T, Sugano Y, Nakayama T, Nagai T, Matsuyama TA, Ohta-Ogo K, Ikeda Y, Ishibashi-Ueda H, Nakatani T, Yasuda S, Takeishi Y, Ogawa H, Anzai T. Significance of myocardial tenascin-C expression in left ventricular remodelling and long-term outcome in patients with dilated cardiomyopathy. *Eur J Heart Fail* 2016; **18**: 375–385.
24. MacIver DH, Adeniran I, Zhang H. Left ventricular ejection fraction is determined by both global myocardial strain and wall thickness. *Int J Cardiol Heart Vasc* 2015; **7**: 113–118.
25. Katz AM. *Heart Failure: Pathophysiology, Molecular Biology, and Clinical Management*. Philadelphia: Lippincott Williams & Wilkins; 2000.
26. Yarbrough WM, Mukherjee R, Brinsa TA, Dowdy KB, Scott AA, Escobar GP, Joffs C, Lucas DG, Crawford FA Jr, Spinale FG. Matrix metalloproteinase inhibition modifies left ventricular remodeling after myocardial infarction in pigs. *J Thorac Cardiovasc Surg* 2003; **125**: 602–610.
27. Ikonomidis JS, Hendrick JW, Parkhurst AM, Herron AR, Escobar PG, Dowdy KB, Stroud RE, Hapke E, Zile MR, Spinale FG. Accelerated LV remodeling after myocardial infarction in TIMP-1-deficient mice: effects of exogenous MMP inhibition. *Am J Physiol Heart Circ Physiol* 2005; **288**: H149–H158.
28. Roten L, Nemoto S, Simsic J, Coker ML, Rao V, Baicu S, Defreyte G, Soloway PJ, Zile MR, Spinale FG. Effects of gene deletion of the tissue inhibitor of the matrix metalloproteinase-type 1 (TIMP-1) on left ventricular geometry and function in mice. *J Mol Cell Cardiol* 2000; **32**: 109–120.
29. Creemers EE, Davis JN, Parkhurst AM, Leenders P, Dowdy KB, Hapke E, Hauet AM, Escobar PG, Cleutjens JP, Smits JF, Daemen MJ, Zile MR, Spinale FG. Deficiency of TIMP-1 exacerbates LV remodeling after myocardial infarction in mice. *Am J Physiol Heart Circ Physiol* 2003; **284**: H364–H371.
30. Tian H, Cimini M, Fedak PW, Altamentova S, Fazel S, Huang ML, Weisel RD, Li RK. TIMP-3 deficiency accelerates cardiac remodeling after myocardial infarction. *J Mol Cell Cardiol* 2007; **43**: 733–743.
31. Li YY, Feldman AM, Sun Y, McTiernan CF. Differential expression of tissue inhibitors of metalloproteinases in the failing human heart. *Circulation* 1998; **98**: 1728–1734.
32. Ducharme A, Frantz S, Aikawa M, Rabkin E, Lindsey M, Rohde LE, Schoen FJ, Kelly RA, Werb Z, Libby P, Lee RT. Targeted deletion of matrix metalloproteinase-9 attenuates left ventricular enlargement and collagen accumulation after experimental myocardial infarction. *J Clin Invest* 2000; **106**: 55–62.
33. Liu YH, Yang XP, Sharov VG, Nass O, Sabbah HN, Peterson E, Carretero OA. Effects of angiotensin-converting enzyme inhibitors and angiotensin II type 1 receptor antagonists in rats with heart failure. Role of kinins and angiotensin II type 2 receptors. *J Clin Invest* 1997; **99**: 1926–1935.
34. Imanaka-Yoshida K. Tenascin-C in cardiovascular tissue remodeling: from development to inflammation and repair. *Circ J* 2012; **76**: 2513–2520.
35. Leenen FH, Skarda V, Yuan B, White R. Changes in cardiac ANG II postmyocardial infarction in rats: effects of nephrectomy and ACE inhibitors. *Am J Physiol* 1999; **276**: H317–H325.
36. Weber KT, Brilla CG. Pathological hypertrophy and cardiac interstitium. Fibrosis and renin-angiotensin-aldosterone system. *Circulation* 1991; **83**: 1849–1865.
37. Sun Y, Cleutjens JP, Diaz-Arias AA, Weber KT. Cardiac angiotensin converting enzyme and myocardial fibrosis in the rat. *Cardiovasc Res* 1994; **28**: 1423–1432.
38. Zou Y, Komuro I, Yamazaki T, Kudoh S, Aikawa R, Zhu W, Shiojima I, Hiroi Y, Tobe K, Kadowaki T, Yazaki Y. Cell type-specific angiotensin II-evoked signal transduction pathways: critical roles of $G_{\beta\gamma}$ subunit, Src family, and Ras in cardiac fibroblasts. *Circ Res* 1998; **82**: 337–345.
39. Li H, Simon H, Bocan TM, Peterson JT. MMP/TIMP expression in spontaneously hypertensive heart failure rats: the effect of ACE- and MMP-inhibition. *Cardiovasc Res* 2000; **46**: 298–306.